

Paper No.
16581



Effect of Steel Microstructure and Corrosion Product Characteristics on Inhibition Performance of Decanethiol Against Top of the Line Corrosion

Z. Belarbi, F. Farelas, D. Young, M. Singer

Institute for Corrosion and Multiphase Technology
Department of Chemical & Biomolecular Engineering
Ohio University
342 West State Street
Athens, OH 45701

ABSTRACT

The use of corrosion inhibitors to control top of the line corrosion (TLC) of steels exposed to CO₂ environments is common in the oil and gas industry. The performance of such chemicals depends on the physical nature of the steel surface and the stability of corrosion product layers. The objective of this work was to investigate and understand the role of steel microstructure (pearlitic-ferritic and tempered martensitic) and the state of a pre-corroded surface, specifically the effect of FeCO₃ and Fe₃C corrosion product layers on the inhibition performance of decanethiol at TLC conditions. Weight loss measurements and Fe²⁺ concentration in condensed water were used to measure the corrosion rate in the absence and presence of decanethiol. Scanning electron microscopy (SEM) coupled with energy-dispersive X-ray spectroscopy (EDS) were used to characterize the morphology and chemical composition of the surface. After the removal of the corrosion products, profilometry was performed to assess the occurrence of localized attack. The acquired data showed that the steel microstructure and the nature of the corrosion product layer affect the inhibition performance of decanethiol in a CO₂ environment. The presence of a FeCO₃ layer decreased the inhibition efficacy of decanethiol (95 to 82%). In contrast, the presence of a Fe₃C layer did not affect the inhibition efficacy of the tested chemical. An inhibition mechanism was also proposed based on the physical properties and the nature of the surface.

Keywords: CO₂ corrosion, iron carbonate, top of the line corrosion, decanethiol, cementite, scale

INTRODUCTION

Chemical composition and microstructure of carbon steel plays an important role in corrosion processes. In 1963, Staicopolus¹ studied the behavior of cementite under cathodic polarization. It was found the cementite can act as a cathodic site, which means that while the ferrite phase dissolves (oxidation reaction), reduction of hydrogen ions happens where the cementite phase is present. In carbon steels, the volumetric quantity of Fe₃C increases with carbon content, thereby affecting the corrosion rate. A twofold increase, or more, in the corrosion rate has been measured on steels when the carbon content is increased from 0.2 to 0.8 wt%.²

Deterioration of carbon steels exposed to aggressive environments, such as those containing CO₂, H₂S and/or organic acids, cannot be avoided. However, it can be mitigated by injection of corrosion inhibitors (CIs). The efficiency of CIs is usually measured by exposing a polished carbon steel specimen to an aggressive environment. By means of electrochemical techniques, the corrosion rate before adding the CI is measured and the efficiency calculated based on the observed corrosion rate after the addition of the CI. However, the presence of corrosion products on the steel surface, such as iron carbonate (FeCO₃), iron sulfide (FeS) and/or iron carbide (Fe₃C) has the potential to affect the efficiency of CIs; Fe₃C is not considered as a corrosion product in the same way as FeCO₃ or FeS, rather it is a residual phase that is exposed after the oxidative dissolution of the ferrite phase). The development of corrosion product layers on carbon steel is known to depend on operating conditions relating to solution pH, temperature, carbon dioxide partial pressure, aqueous speciation, ionic strength, dissolved oxygen level, hydrodynamics and the steel microstructure.³ Therefore, it is important to study the efficiency of corrosion inhibitors on steel specimens that have been pre-corroded in order to investigate the effect of microstructure and corrosion products on inhibitor performance.

Some researchers have reported that the performance of CIs can be impaired by the presence of a carbide layer. Gulbrandsen *et al.*⁴ tested the efficiency of six commercial inhibitors (imidazolines and amines) at different pre-corrosion times. It was found that the inhibitor's efficiency decreased with an increase in the pre-corrosion time due to the presence of a cementite layer. According to the authors, with longer pre-corrosion times, the inhibition kinetics became slower but no further explanation was given. Recently, Xiong *et al.*⁵ studied the impact of pre-corrosion on steel with a pearlitic-ferritic microstructure. Similar to what Gulbrandsen *et al.* found, Xiong *et al.* reported a decrease of the inhibitor efficiency with the pre-corrosion duration, an effect that was possible to counteract with an increase of inhibitor concentration. Kapusta, *et al.*⁶ found that 1 day of pre-corrosion had a negative effect on inhibitor performance. However, Dougherty, *et al.*⁷ found that certain oil soluble inhibitors performed better on pre-corroded surfaces. Liu *et al.*⁸ investigated the inhibition performance of thioglycolic acid (TGA), diethylenetriamine (DETA), and naphthenic acid imidazolines (IM), on the bare surface of N80 steel and its scaled surface pre-corroded in CO₂-saturated 1 wt.% NaCl solution. It was found that IM and DETA have a positive synergistic effect with the corrosion scale formed on N80 steel. However, TGA shows good inhibition efficiency on bare N80 steel. The author showed that the inhibition performance depends on the size of inhibitor molecule and its interaction with the corrosion product. In another study⁹, the inhibition performance of the amine-based inhibitor on iron carbonate was superior at lower concentration than at higher concentration.

Many studies have discussed the influence of chemical composition and microstructure of carbon steels on inhibitor performance.^{4,10,11} Lopez *et al.*^{12,13} evaluated the effect of the addition of 100 ppm of benzimidazole in the presence of corrosion product layers obtained on ferritic-pearlitic and martensitic microstructures of a J55 carbon steel. The authors concluded that the microstructure of the steel

influences the inhibitor efficiency, as well as the morphology and chemical composition of the corrosion product layers.

However, most of these studies did not give a clear explanation relating microstructure, pre-corrosion and chemical composition of steel to corrosion inhibition mechanisms in CO₂ environments. Heretofore, there is no research reported in the open literature about the effect of pre-corrosion on the efficacy of volatile corrosion inhibitors. The objective of this paper is to evaluate the effect of the steel surface (steel type, microstructure and corrosion product layers (Fe₃C, FeCO₃)) on the efficacy of decanethiol, proven to be an effective volatile inhibitor for TLC on non-pre-corroded mild steel surface exposed to CO₂ environment.¹⁴ Belarbi *et al.*¹⁵ investigated the inhibition mechanism of CO₂ corrosion by decanethiol and discussed the anodic and cathodic reaction inhibition using electrochemical measurements. The author was able to propose a mechanism of adsorption of decanethiol using electrochemical techniques and surface analysis (specifically XPS).

EXPERIMENTAL PROCEDURE

Materials and Chemicals

The specimens used in the corrosion inhibition experiments were made of an API⁽¹⁾ 5L X65 carbon steel with a tempered martensitic microstructure and a 1018 (UNS G10180) steel with a ferritic-pearlitic microstructure. Figure 3 and Figure 4 show SEM images at different magnifications of the etched surface. The 1018 steel microstructure consists of two phases (α -ferrite and cementite) organized between grains of ferrite and colonies of pearlite. The pearlite microconstituent has a lamellar structure with cementite (white) and ferrite (gray) lamellae (Figure 1). However, the API X65 carbon steel microstructure consists of ferrite with cementite precipitates at the grain boundaries (Figure). The chemical compositions of each steel are given in Table 1 and Table 2.

The samples were machined into a cylindrical shape, with a diameter of 3.151 cm and 1.146 cm in height. One of the faces and sides were covered with Xylan® coating, leaving an exposed area of 7.79 cm². Decanethiol used in this research was acquired from Sigma-Aldrich‡.

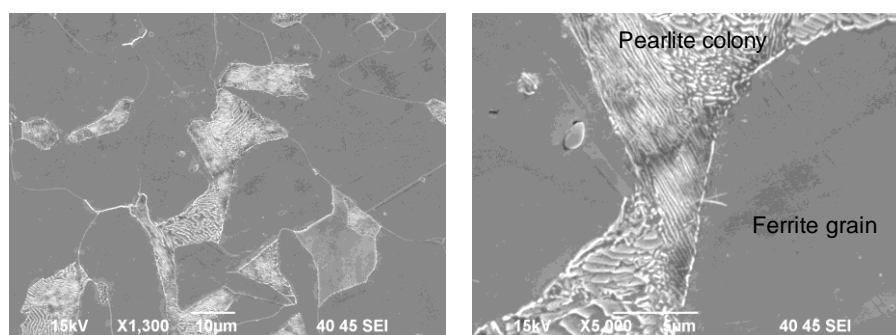


Figure 1. Microstructure of the 1018 carbon steel, 30 second etch in 2% Nital solution

‡ Trade name

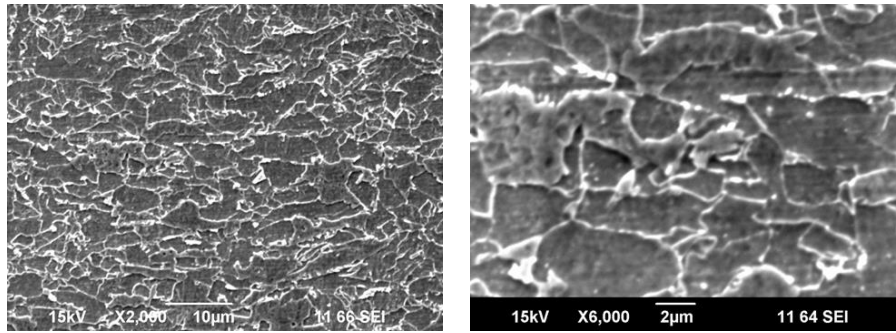


Figure 2. Microstructure of the API 5L X65 carbon steel, 30 second etch in 2% Nital solution

Table 1. Composition (wt.%) of API⁽¹⁾ 5L X65 carbon steel

Element	C	Nb	Mn	P	S	Ti	V	Ni	Fe
X65	0.05	0.03	1.51	0.004	<0.001	0.01	0.04	0.04	balance

Table 2. Composition (wt.%) of 1018 carbon steel

Element	C	Nb	Mn	P	S	Ti	V	Ni	Cr	Cu	Mo	Al	Fe
1018	0.17	0.002	0.66	0.007	0.02	0.001	0.002	0.06	0.073	0.14	0.04	0.04	balance

Weight loss measurements

The experimental setup consisted of a 4 L glass cell that was designed for top of the line corrosion experiments. Figure shows different views of the TLC glass cell. A 1 wt.% NaCl electrolyte (2.5 l) was placed in the glass cell and sparged with CO₂ for 2 hours to deoxygenation and ensure saturation. A hot plate allowed for the heating of the bottom solution to 74°C and the gas temperature to 65°C. In order to facilitate different water condensation rates, the weight loss (WL) specimens were heated or cooled by circulating a glycol solution through specimen heating/cooling systems. A circulating bath was used to control the glycol temperature. On the lid, a WL specimen was flush mounted, allowing their exposure to the wet gas phase. WL specimens were mechanically polished using silicon carbide paper (180, 400 and 600 grit), cleaned with isopropanol in an ultrasonic bath for 5 minutes, and dried at room temperature before introduction into the glass cell. Gas, steel temperature and solution pH were monitored during the experiment. A 45 ml cup was placed just below a WL sample and was used to collect the condensed water every 12 – 24 h, enabling calculation of the water condensation rate. In addition, the iron concentration was measured with a spectrophotometer.

WL Corrosion rate of the specimen at the top (TLC rate) with and without the addition of inhibitors was measured following the ASTM⁽²⁾ G1 standard.¹⁶ The detailed TLC experimental matrix for the experimental work is shown in Table 3 and Table 4. In order to investigate the inhibition performance of decanethiol in the presence of corrosion products, carbon steel specimens were pre-corroded in the glass cell at lower temperature (to avoid FeCO₃ precipitation) for 2 days to form cementite or at higher temperature for 7 days to form iron carbonate. The experimental procedure used for investigating the inhibition performance of decanethiol in the presence of corrosion products under TLC conditions is shown in Figure 4.

⁽¹⁾ American Petroleum Institute (API), 1220 L St. NW, Washington, DC 20005.

⁽²⁾ American Society for Testing and Materials (ASTM), 100 Barr Harbor Drive, West Conshohocken, PA, 19428-2959.

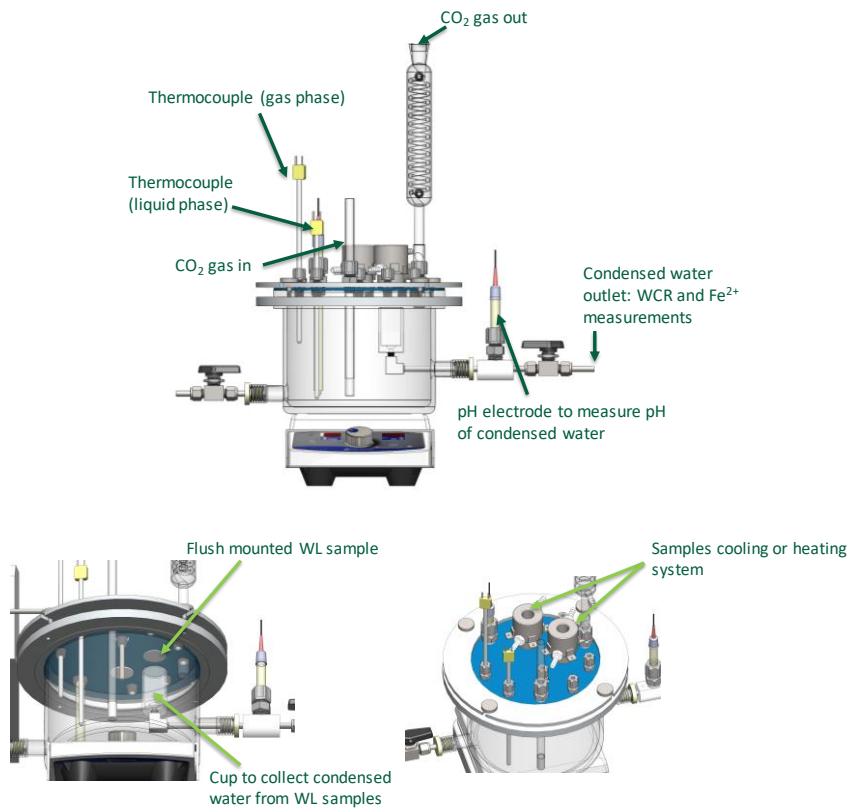


Figure 3. Top of the line corrosion glass cell system

Table 3. Experimental parameters to test the effect of microstructure and carbon content on the inhibition efficiency of decanethiol

Total pressure (bar)	1	
pCO ₂ (bar)	0.66	
Solution	2.5 l of 1 wt.% NaCl	
Solution temperature at the bottom	74 ± 2°C	
Gas temperature	~ 65 ± 1°C	
Sample temperature	~ 56 ± 1°C	
Measured water condensation rate (ml/m ² /s)	~ 0.50	~ 0.28
decanethiol (ppm _v)	0	400
Working electrode	X65 carbon steel 1018 carbon steel	
Acetic acid (ppm _v)	600	
Duration (day)	2, 4	

Table 4. Experimental parameters to test the effect of FeCO₃ on the inhibition efficiency of decanethiol

Total pressure (bar)	1	
pCO ₂ (bar)	0.66	
Solution	1 wt.% NaCl	
Solution temperature at the bottom	74 ± 2°C	
Gas temperature	~ 66 ± 1°C	
Sample temperature	~ 63 ± 1°C	
Measured water condensation rate (ml/m ² /s)	~ 0.43	~ 0.2
decanethiol (ppm _v)	0	400
Working electrode	1018 carbon steel	
Duration (day)	7, 14	

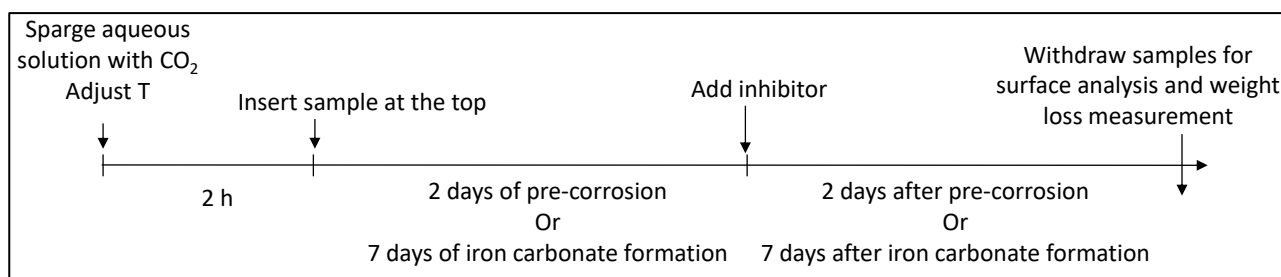


Figure 4. Experimental procedure used for investigating the inhibition performance of decanethiol on FeCO₃ covered and pre-corroded surfaces

Surface analysis

Scanning electron microscopy (SEM, JEOL JSM-6090 LV) and an EDAX energy dispersive X-ray spectroscopy (EDS) system were used to characterize surface morphology and perform the chemical analysis of the exposed specimens. Imaging was performed at an accelerating voltage of 15 kV using a secondary electron detector (SEI). Surface profile analysis was performed using a profilometer (Alicona) to investigate the extent of localized corrosion.

RESULTS AND DISCUSSION

Effect of microstructure and carbon content on decanethiol inhibition efficacy

In this study, two different steel microstructures and steel chemical compositions (1018 and X65) were used to evaluate the inhibition performance of decanethiol in TLC conditions (Table 3). The pH profile of the condensed water and TLC rate based on Fe²⁺ measurements in the condensed water with and without decanethiol are shown in Figure 5 and Figure 6. The pH of the condensed water is an important parameter determining the corrosivity of the aqueous phase in contact with the steel surface. Without decanethiol, the measured steady state pH was around 5.4 for the X65 carbon steel and 5.6 for the 1018 (Figure 5). The high pH in the condensed water was due to the presence of Fe²⁺ coming from the steel samples as a reflection of the extent of corrosion (Figure 6). With decanethiol the pH remained around 3.4 for X65 and 4.1 for 1018, as shown in Figure 5. These values are similar to the estimated pH of the

pure condensed water (dash horizontal line on Figure 5), which is 3.4 at the experimental conditions. Therefore, the decrease of the pH is due to the low corrosion rate (Figure 6) (low Fe^{2+} release), knowing that the injection of decanethiol has no effect on the solution pH. These results indirectly suggest that decanethiol is protecting the X65 and 1018 steel surfaces.

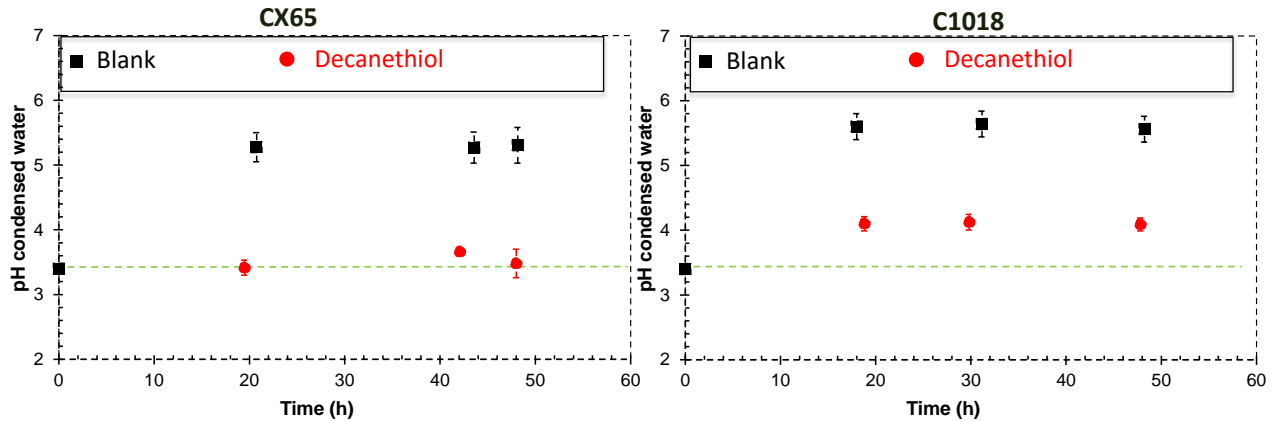


Figure 5. pH profile of CO_2 -saturated condensed water with and without decanethiol
The dotted line indicates the pH of freshly condensed water

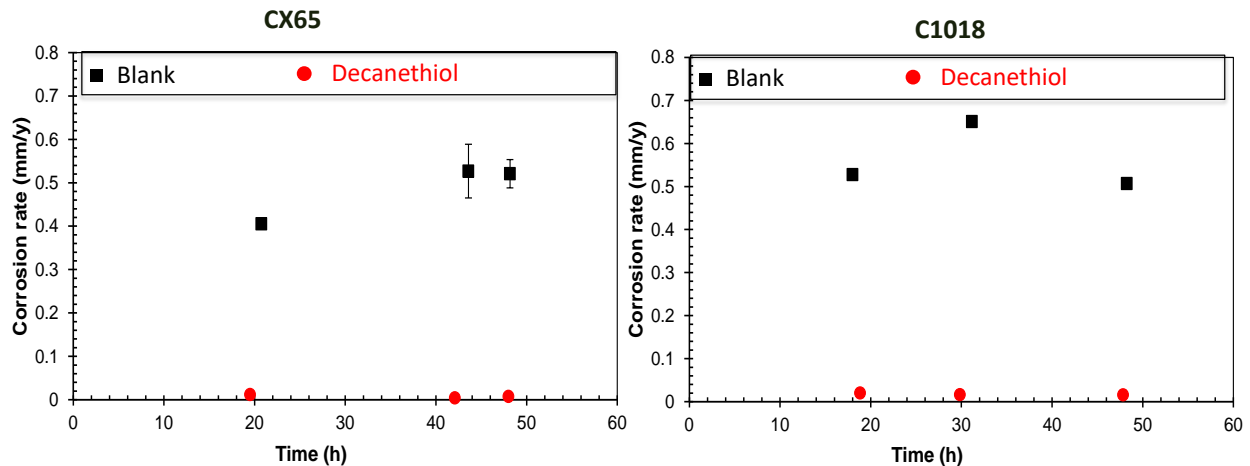


Figure 6. *In situ* TLC rate based on Fe^{2+} measurements in CO_2 -saturated condensed water with and without decanethiol

TLC weight loss corrosion rates are compared in Figure 7 to TLC rate based on Fe^{2+} measurements for the 1018 and X65 carbon steel specimens exposed to CO_2 -saturated condensed water with and without decanethiol. The results show that for the baseline conditions, the X65 and 1018 carbon steel specimens corroded at an average TLC rate of 0.74 mm y^{-1} . In the presence of decanethiol the corrosion rate decreased by an order of magnitude, to reach a value lower than 0.07 mm y^{-1} . With regard to the microstructure and chemical composition, with and without decanethiol, both steels behaved similarly. Images corresponding to the surfaces for the 1018 and X65 specimens after 2 days of exposure to the TLC corrosive media, with and without decanethiol, are shown in Figure 8 and Figure 9, respectively. The 1018 microstructure consists of ferrite ($\alpha\text{-Fe}$) and pearlite (lamellar structure containing cementite (Fe_3C) with $\alpha\text{-Fe}$) grains. In the absence of decanethiol, the ferrite phase was dissolved leaving behind a residual Fe_3C layer derived from the original pearlite microconstituent (Figure 8a). As the corrosion process continues, more Fe_3C is revealed on the surface. However, for the X65, the cementite phase (Fe_3C) accumulated and spreads on the metal surface after preferential dissolution of the ferrite phase.

Therefore, the X65 carbon steel surface was fully covered by discrete residual Fe_3C (Figure 9). The corrosion product is assumed to be mainly an iron carbide layer because the EDS analysis (the EDS spectra are not shown in this manuscript) for the X65 and 1018 revealed mainly Fe, C and residual alloying elements on the surface. In the presence of decanethiol, no corrosion was apparent on the X65 carbon steel specimen (Figure 9) and only minimally corroded areas were observed on the 1018 carbon steel (Figure 8b and Figure 8c). For both steels the surface was protected. The analyzed data show that the steel microstructure and its chemical composition have a minor effect on the inhibition performance of decanethiol. Belarbi, *et al.*^{15, 16} discussed the possible interactions between the X65 carbon steel surface and decanethiol. It was found that decanethiol physisorbs on the surface forming monolayer or bilayer structures and thereby retards the both anodic and cathodic reactions.

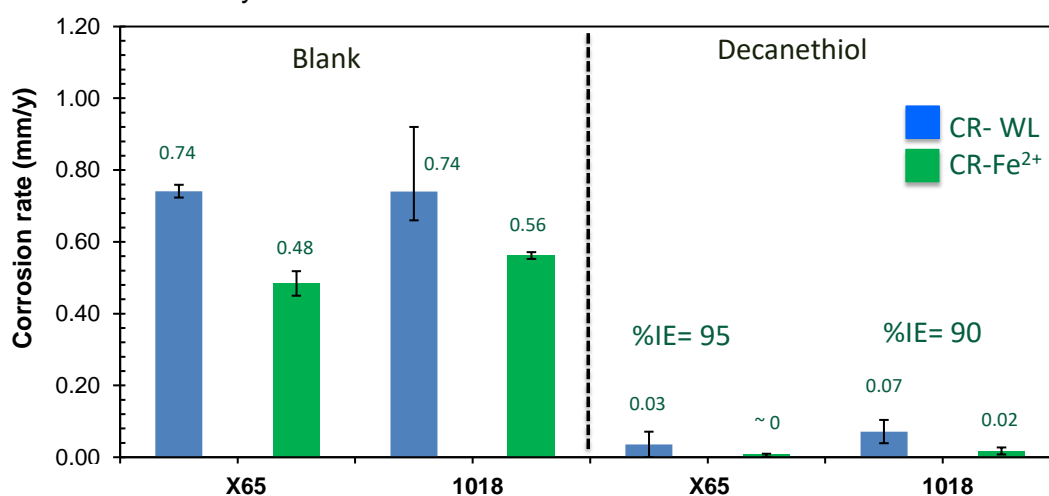


Figure 7. TLC Weight loss corrosion rates of 1018 and X65 carbon steels in CO_2 -saturated condensed water with and without decanethiol

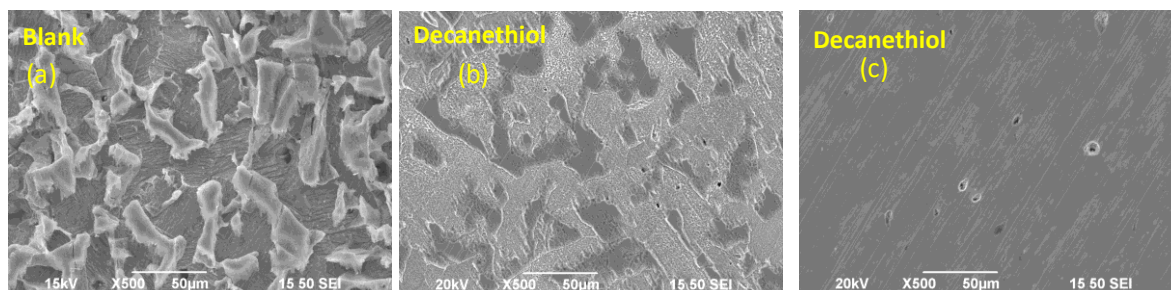


Figure 8. Surface analysis of 1018 carbon steel after 2 day of exposure to the TLC corrosive media with (b, c) and without decanethiol (a).

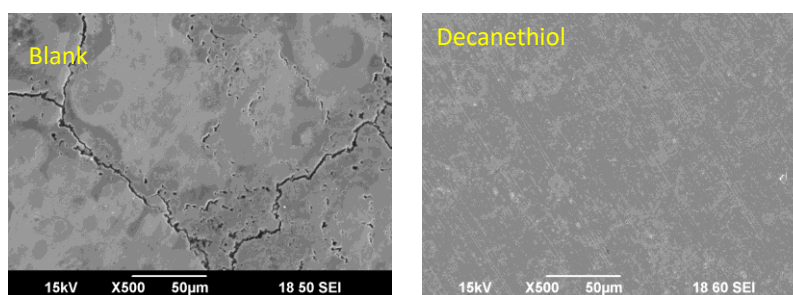


Figure 9. Surface analysis of X65 carbon steel after 2 day of exposure to the TLC corrosive media with and without decanethiol

Effect of pre-corrosion on decanethiol inhibition efficacy

The inhibitor performance on pre-corroded surface might differ significantly from what is seen on bare carbon steel surfaces. For this reason, it is important to investigate the performance of decanethiol on a pre-corroded 1018 carbon steel surface (Table 3). The pH profile and *in situ* TLC rate based on Fe^{2+} measurements in the condensed, water with and without decanethiol, of pre-corroded 1018 carbon steel are shown in Figure 10. During the two day pre-corrosion period, the pH of condensed water was around 5.6. The high pH in the condensed water was due to reduction of hydrogen ions and dissolution of iron. After injection of 400 ppm_v decanethiol (at the bottom solution), the pH of the condensed water decreased to reach a value of 3.4. The decrease of the pH is an indication of mitigation of hydrogen ion reduction and consequent less release of Fe^{2+} (decrease in corrosion rate). The weight loss corrosion rates obtained after 2 days of pre-corrosion in the presence of 400 ppm_v decanethiol are reported in Figure 11. On freshly polished steel the corrosion rate observed with decanethiol was 0.07 mm y⁻¹. However, on the pre-corroded surface the overall corrosion rate increased to 0.45 mm y⁻¹ (Figure 11a). In order to evaluate the effect of decanethiol, the weight loss during the pre-corrosion period was subtracted from the overall weight and the corrosion rate considering only the period after adding inhibitor was evaluated around 0.2 mm y⁻¹. This meant that on the pre-corroded surface, corrosion efficiency of decanethiol decreased from 90% to 77%. The decrease of decanethiol performance could be due to either the increase of cathodic area (Fe_3C) that is affecting the cathodic reactions or to an electrochemical potential gradient between the Fe_3C pores (PZC of the surface) that prevented decanethiol from adsorbing on the steel surface. Fe_3C has been shown to be a very efficient substrate for H_2 evolution in acidic solutions.¹ It has been reported in the literature^{15,17} that the steel surface is positively charged in acidic environments, based on potential of zero charge (PZC) measurements; therefore, the adsorption of anions or molecules possessing permanent dipoles is considered likely. However, with pre-corrosion, the PZC might have been changed and Fe_3C may thus possess different surface-chemical properties than ferrite. Therefore, a systematic study is needed to identify the PZC of pre-corroded steel exposed to TLC conditions. SEM surface analysis of the pre-corroded surface with and without decanethiol is shown in Figure 12.

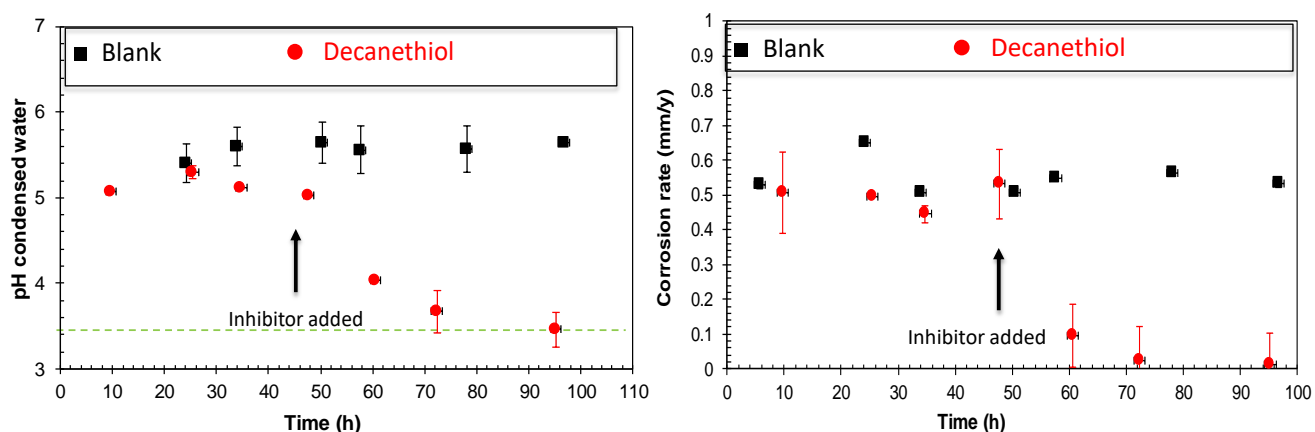


Figure 10. The pH profile and *in situ* TLC rate based on Fe^{2+} measurements in the CO_2 -saturated condensed water with and without decanethiol for pre-corroded 1018 carbon steel

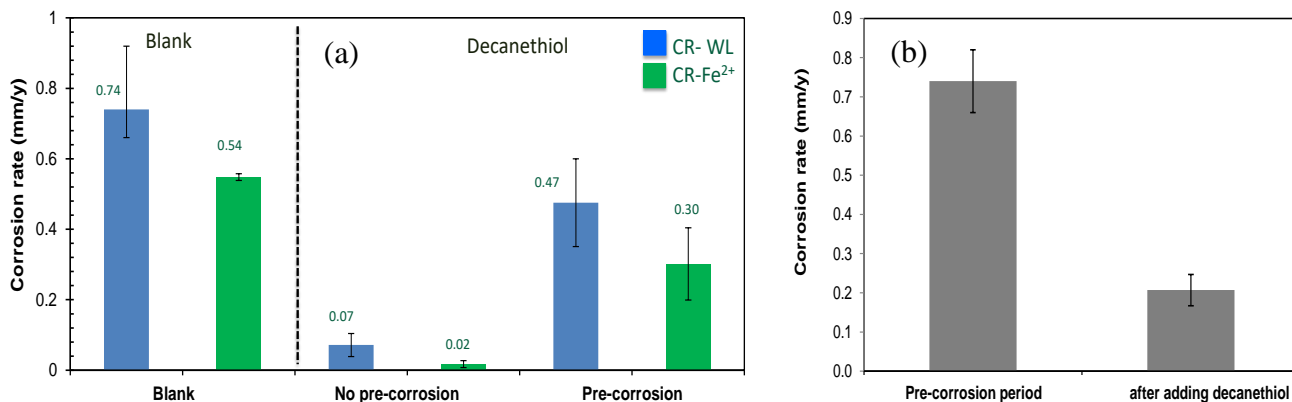


Figure 11. TLC Weight loss corrosion rates of 1018 carbon steel in CO₂-saturated condensed water with and without pre-corrosion in the absence and presence of decanethiol. a). The overall corrosion rates with pre-corrosion period. b). Corrosion rates after subtraction of pre-corrosion period

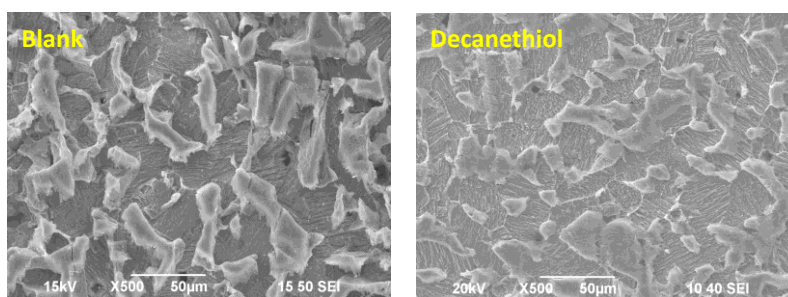


Figure 12. Surface analysis of 1018 carbon steel after 2 day pre-corrosion of exposure to the TLC corrosive media with and without decanethiol

Effect of iron carbonate on decanethiol inhibition efficacy

It has been reported that iron carbonate can slow down the corrosion process by acting as barrier to transportation of corrosive species^{18,19}, and the corrosion products may reduce access of the inhibitor to the steel surface.⁸ Therefore, it is important to study the effect of this corrosion product on inhibition efficacy. The iron carbonate layer was formed on 1018 carbon steel in CO₂-saturated condensed water under TLC conditions (Table 4).

The pH profile and *in situ* TLC rate based on Fe²⁺ measurements in the condensed water with and without decanethiol in the presence and absence of iron carbonate on 1018 carbon steel are shown in Figure 13 and Figure 14, respectively. In the absence of decanethiol, the pH of condensed water was around 5.9. In the presence of decanethiol, the pH of condensed water decreased to reach a value of 5 (Figure 13). As described previously, the decrease of the pH is an indication of mitigation of hydrogen ion reduction and less release of Fe²⁺ (decrease in corrosion rate, Figure 14). The corrosion rates obtained by the weight loss measurements are shown in Figure 15. The results show that, for the baseline conditions, the 1018 specimen was corroded at a TLC rate of 0.51 mm y⁻¹ and its surface was fully covered by a corrosion product (Figure 16). On bare steel and in the presence of decanethiol, the corrosion rate decreased from 0.5 to 0.03 mm y⁻¹ and the inhibitor showed an efficacy of 95 % (Figure 15 a). However, for the specimen pre-corroded (covered with FeCO₃) and treated with decanethiol, the corrosion rate was 0.3 mm y⁻¹; which is lower than the blank (Figure 15 a). This result indicates that decanethiol can decrease the corrosion rate in the presence of the corrosion product. The corrosion rate that was calculated from free iron concentration in condensed water was also lower than the weight loss corrosion rate (0.03 compared to 0.3 mm y⁻¹). That indicates that there was precipitation of iron

carbonate on the steel surface and that most iron loss from corrosion ended up in the corrosion product layer. To estimate the inhibition efficacy of decanethiol, the weight loss during the pre-corrosion period (7 days) was subtracted from the overall weight (14 days) and the corrosion rate considering only the period after adding inhibitor was calculated to be ca. 0.06 mm y⁻¹ (Figure 15 b). Based on weight loss corrosion rate of FeCO₃ covered scale surface (Figure 15), corrosion efficiency of decanethiol decreased from 95% to 82 %.

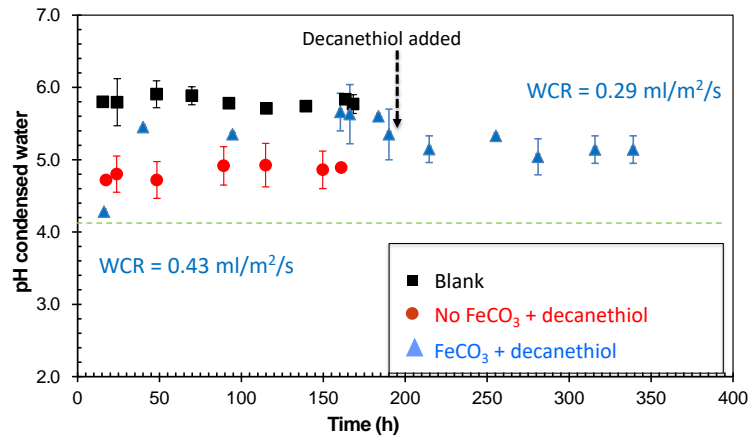


Figure 13. The pH profile of CO₂-saturated condensed water with and without decanethiol under corrosion product formation conditions

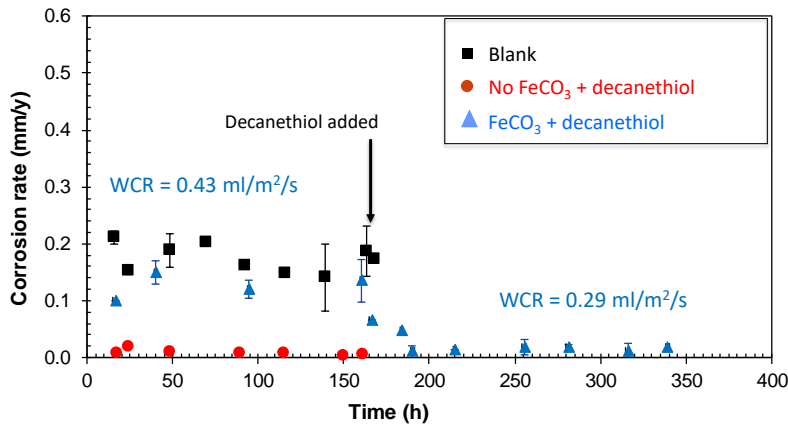


Figure 14. *In situ* TLC rate based on Fe²⁺ measurements of pre-corroded 1018 carbon steel in CO₂-saturated condensed water with and without decanethiol under corrosion product formation conditions

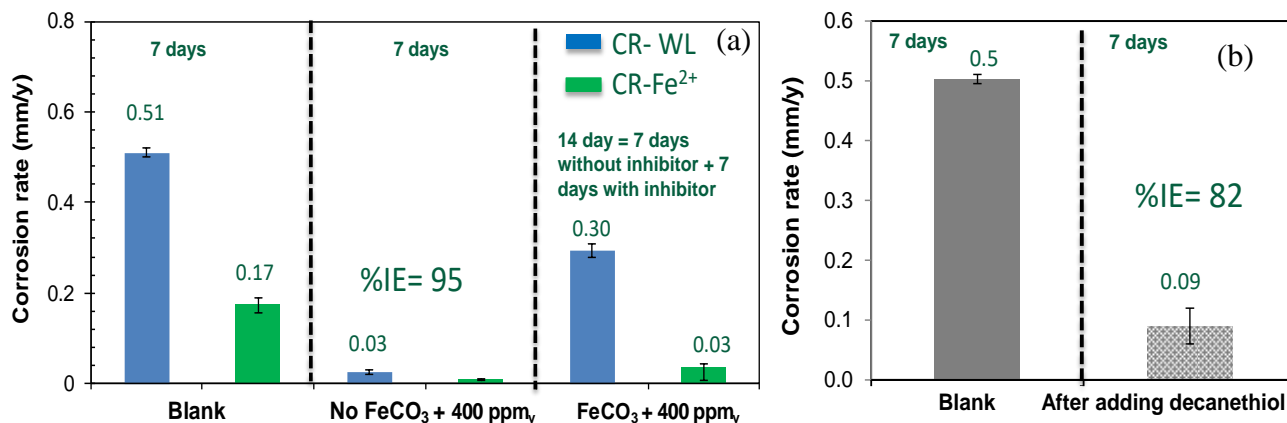


Figure 15. TLC Weight loss corrosion rates of 1018 carbon steel in CO₂-saturated condensed water with and without FeCO₃ in the absence and presence of decanethiol: a). The overall corrosion rates with FeCO₃; b). Corrosion rates after subtraction of pre-corrosion period

Figure 16 shows the surface morphology and EDS cross-section analysis of corrosion products formed on the 1018 mild steel surface in CO₂-saturated condensed water under TLC conditions without decanethiol. The crystal shape and size of the corrosion products are similar to a crystalline ferrous carbonate layer (FeCO₃). EDS cross-section analysis detected Fe, O and C which suggested the likely presence of an iron carbonate layer. Figure 17a shows the SEM images and EDS analysis of the bare 1018 steel and corrosion products formed on the steel surface in CO₂-saturated condensed water under TLC conditions with decanethiol. No corrosion product was observed on the steel specimens exposed to decanethiol, and SEM images show the different depths of the mechanical polishing lines on the substrate surface (indicating very low metal loss). EDS analysis did not detect oxygen, which is the dominant chemical element within FeCO₃ on a mole basis.

However, for the specimen pre-corroded (covered with FeCO₃) and treated with decanethiol, SEM results (Figure 17b, Figure 17c) showed that the morphology of the iron carbonate was modified by the presence of the inhibitor. An obvious change was noted in the distribution, size and morphology of the FeCO₃ precipitate; the crystals lost their sharp edges, became distorted, and their size was larger than those deposited in uninhibited solution. This may be due to the interaction of the decanethiol with the corrosion product layer (FeCO₃) or to the adsorption of decanethiol on the steel surface, which decreases the rate of release of Fe²⁺. Therefore, the condensed water could become under saturated with respect to FeCO₃. It is generally accepted that the inhibition of corrosion product formation is influenced by the inhibitor molecules adsorbed on the FeCO₃ crystal surface and on the steel substrate. These results indicate that there is a remarkable difference in inhibition efficiency of decanethiol on the 1018 steel with and without a corrosion product layer.

The surface morphology of 1018 carbon steel after removing the corrosion product layers was characterized by profilometry (IFM). Figure 18 shows the surface profile of the corroded specimens with and without decanethiol. In the absence of decanethiol, the depth of the deepest pit on the surface was about 27 micrometers after the 7 day experiment corresponding to a localized corrosion rate of 1.46 mm y⁻¹, while the general corrosion rate by weight loss of this sample (Figure 15) was only 0.5 mm y⁻¹. However, in the presence of decanethiol, the general and localized corrosion rates were 0.31 mm y⁻¹ and 0.78 mm y⁻¹, respectively. In both cases, with and without decanethiol, the pitting ratio between the localized corrosion and general corrosion was below 2.8. By comparison, in the presence of decanethiol and in the absence of FeCO₃, the general and localized corrosion rates were 0.03 mm y⁻¹ and 0.1 mm y⁻¹, respectively. All these values are too low to be considered as localized corrosion.

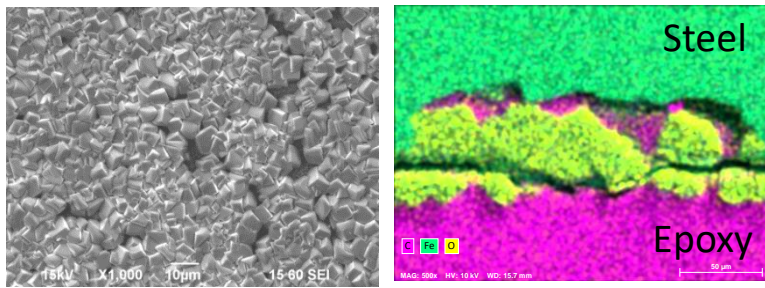


Figure 16. SEM analysis and EDS cross section analysis of the scale formed on 1018 carbon steel in CO_2 -saturated condensed water under TLC conditions

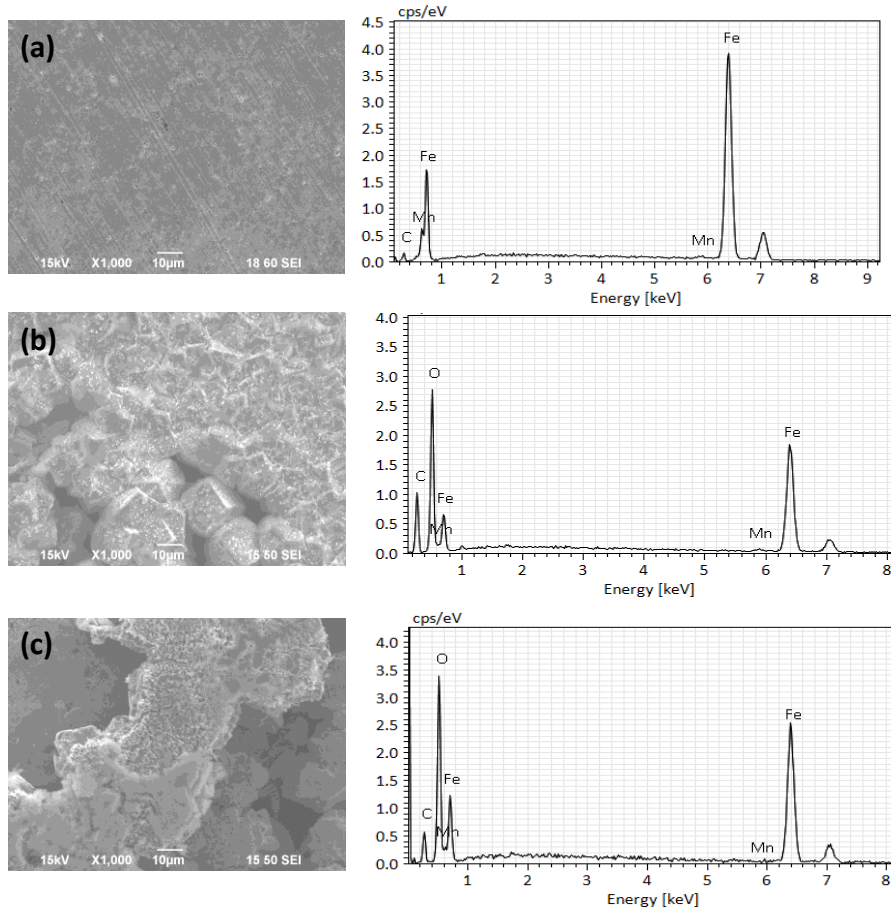


Figure 17. SEM analysis and EDS analysis of 1018 carbon steel in CO_2 -saturated condensed water in presence of decanethiol. a) Bare steel. b) and c) Steel with FeCO_3 layer in two different locations

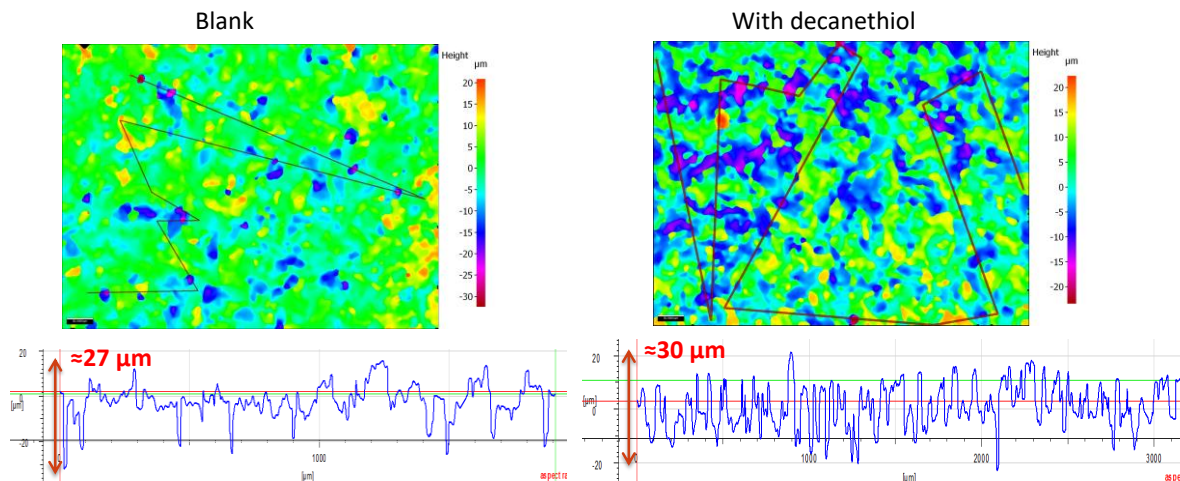


Figure 18. Profilometry analysis of 1018 carbon steel in CO₂-saturated condensed water with FeCO₃ in absence and presence of decanethiol

CONCLUSIONS

The effects of steel microstructure, composition and corrosion products on the inhibition of CO₂ corrosion under TLC conditions have been studied. Based on the weight loss measurements, iron concentrations and SEM analysis, the following conclusions were drawn:

- Decanethiol showed a similar protection on 1018 and X65 carbon steel. Inhibition efficacy was not influenced by the nature or microstructure of the steel (API 5L X65, 1018).
- Laboratory experience shows that inhibitors perform differently on corroded surfaces and freshly polished surfaces. In the presence of Fe₃C the inhibition efficacy of decanethiol decreased from 90% to 77%. The decrease of decanethiol performance could be due to either the increase of cathodic area (Fe₃C) that is affecting the cathodic reactions or to an electrochemical potential gradient between the Fe₃C pores that prevented decanethiol from adsorbing on the steel surface.
- The inhibition of corrosion product formation is influenced by the inhibitor molecules adsorbed on the FeCO₃ crystal surface and on the steel substrate. The adsorption of the decanethiol on the crystal surface caused a deformation of the crystal morphology.

ACKNOWLEDGMENTS

The authors would like to thank the following companies for their financial support: ARKEMA, SHELL, SAUDI ARAMCO, PTTEP and SCHLUMBERGER. The technical support from the lab's staff at Institute for corrosion and multiphase technology by Mr. Alexis Barxias, Mr. Cody Shafer is highly appreciated.

REFERENCES

1. D. N. Staicopolus, "The role of cementite in the acidic corrosion of steel", *Journal of Electrochemical Society*, 110 (11) (1963): pp.1121-1124.
2. S. Al-Hassan, B. Mishra, D. Olson, M. Salama, "Effect of microstructure on corrosion of steels in aqueous solutions containing carbon dioxide", *Corrosion*, 54 (6) (1998): pp. 480-491.
3. M. Cabrini, G. Hoxhra, A. Kopliku, L. Lazzari, "Prediction of CO₂ corrosion in oil and gas wells. Analysis of some case histories", *CORROSION* 1998, paper no. 24 (Houston, TX: NACE, 1998).
4. E. Gulbrandsen, S. Nestic, A. Stangeland, T. Burchardt, "Effect of precorrosion on the performance of

- carbon steel”, CORROSION 1998, paper no. 13 (Houston, TX: NACE ,1998).
5. Y. Xiong, F. Cao, D. Fischer, J. Pacheco, “Impact of pre-corrosion on corrosion inhibitor performance: can we protect aged pipelines”, CORROSION 2017, paper no. 8919 (Houston, TX: NACE, 2017).
 6. S.D. Kapusta, P. R. Rhodes, S. A. Silverman, “Inhibitor Testing for CO₂ Environments”, CORROSION 1991, paper no. 471 (Houston, TX: NACE ,1991).
 7. J. A. Dougherty, D. W. Stegmann, “The Effects of Flow on Corrosion Inhibitor Performance”, CORROSION 1995, paper no. 113 (Houston, TX: NACE, 1995).
 8. D. Liu, Y. B. Qiu, Y. Tomoe, K. Bando, X. P. Guo, “Interaction of inhibitors with corrosion scale formed on N80 steel in CO₂-saturated NaCl solution”, *Materials and Corrosion*, 62 (2) (2011): pp. 1153-1158.
 9. H. Malik, “Influence of C16 quaternary amine on surface films and polarization resistance of mild steel in carbon dioxide-saturated 5% sodium chloride”, *Corrosion*, 51 (4) (1995): pp. 321-328.
 10. S. Nestic, J. Postlethwaite, M. Vrhovac, “CO₂ corrosion of carbon steel. From mechanistic to empirical modelling”, *Corrosion Reviews*, 15 (1-2) (1997): pp. 211-240.
 11. E. Gulbrandsen, R. Nyborg, T. Loland, K. Nisancioglu, “Effect of steel microstructure and composition on inhibition of CO₂ corrosion”, CORROSION 2000, paper no. 23 (Houston, TX: NACE , 2000).
 12. D.A. Lopez, W. H. Schreiner, S. R. de Sanchez, S. N. Simison, “The influence of carbon steel microstructure on corrosion layers. An XPS and SEM characterization”, *Applied Surface Science*, 207 (1-4) (2003): pp. 69-85.
 13. D.A. Lopez, S.N. Simison, S. R. de Sanchez, “The influence of steel microstructure on CO₂ corrosion. EIS studies on the inhibition efficiency of benzimidazole”, *Electrochimical Acta*, 48 (7) (2003): pp. 845-854.
 14. Z. Belarbi, F. Farel, D. Young, M. Singer, S. Nestic, “Thiols as volatile corrosion inhibitors for top-of-the-line corrosion”, *Corrosion*, 73 (7) (2017): pp. 892-899.
 15. Z. Belarbi, J.M. Dominguez Olivo, F. Farel, D. Young, M. Singer, S. Nestic, “Decanethiol as a corrosion inhibitor for carbon steels exposed to aqueous CO₂”, *Corrosion*, 75 (10) (2019): pp. 1246-899.
 16. "Standard practice for preparing cleaning and evaluating corrosion test specimens," ASTM-G1, pp. 15-21, 1999.
 17. Z. Belarbi, F. Farel, D. Young, M. Singer, S. Nestic, “Role of amines in the mitigation of CO₂ Top of the Line Corrosion”, *Corrosion*, 72 (10) (2019): pp. 1300-1310.
 18. S.D. Zhu, A.Q. Fu, J. Miao, Z.F. Yin, G.S. Zhou, J.F. Wei, “Corrosion of N80 carbon steel in oil field formation water containing CO₂ in the absence and presence of acetic acid”, *Corrosion Science*, 53 (2011): pp.3156–3165.
 19. H. Mansoori, D. Young, B. Brown, S. Nestic, M. Singer, “Effect of CaCO₃-saturated solution on CO₂ corrosion of mild steel explored in a system with controlled water chemistry and well-defined mass transfer conditions”, *Corrosion Science* 158 (2019)108078: pp.1–12.